On Energy and Angular Distributions of Electrons in Triplet Production

Eberhard Haug

Lehrstuhl für Theoretische Astrophysik der Universität Tübingen

Z. Naturforsch. **40 a,** 1182–1188 (1985); received September 27, 1985

The differential cross section of electron pair production in the field of free electrons (triplet production) is derived from the cross section for electron-positron bremsstrahlung exact to lowest order of perturbation theory. It is used to compute energy and angular distributions of the outcoming electrons. The results are compared with previous calculations. In particular, the accuracy of the momentum distribution according to the Borsellino approximation is discussed.

1. Introduction

Electron-positron pair production in the field of an electron, often referred to as triplet production, is a fundamental process of quantum electrodynamics. In lowest-order perturbation theory it is described by eight Feynman diagrams [1]. Therefore the expressions for the cross sections are much more complicated than the familiar Bethe-Heitler formulae for pair production in the static Coulomb field of an atomic nucleus [2]. The fully differential cross section for pair production in the field of unpolarized electrons by unpolarized photons was first derived by Votruba [3]. This extremely lengthy expression can be greatly reduced by neglecting the four exchange diagrams and the interaction of the incident photon with the target electron, the so-called $\gamma-e$ interaction [4]. This approximation, worked out by Borsellino [5] and Ghizzetti [6], yields accurate results at high photon energies [4]. Near threshold, however, the consideration of exchange leads to a reduction of the available phase space corresponding to a strong overestimation of the cross section by the Borsellino formula [4]. Kopylov et al. [7], Mork [8], and Jarp and Mork [9] used the Monte Carlo method to integrate the fully differential cross section, confirming that the triplet production at high photon energies is well represented by the Borsellino formula. Mork [8], in particular, investigated separately the contributions of the different Feynman diagrams and their interferences. Haug [10] succeeded in calculating the doubly differential cross section of electron-electron bremsstrahlung which is exact in lowest-order perturbation theory. Turning to the triplet production via the substitution rule [1] this expression gives the angular distributions of the produced *positrons* in arbitrary frames of reference. The positron spectra could be obtained from this formula by a single numerical integration. The calculation of the total cross section for triplet production requires two numerical integrations, resulting in higher accuracy compared with the former Monte Carlo computations.

Recently a formula for the doubly differential cross section of electron-positron bremsstrahlung was derived [11]. It is also exact in lowest-order perturbation theory and is expressed as a function of invariant products so that it can be specialized to any frame of reference. According to the substitution rule the process of electron-positron bremsstrahlung corresponds to triplet production where one of the outgoing *electrons* is observed. Thus it is now possible to compute energy and angular distributions of the electrons by simple numerical integrations. In this paper the results of these calculations are compared with previous work. In particular the different behaviour of the electron momentum distributions as against the results of the Borsellino formula is demonstrated.

2. Triplet Cross Section

In the elementary process of triplet production (Fig. 1) a photon with four-momentum $\mathbf{k} = (k, \boldsymbol{k})$ *

Reprint requests to Dr. E. Haug, Lehrstuhl für Theoretische Astrophysik der Universität Tübingen, Auf der Morgenstelle 12, D-7400 Tübingen, FRG.

* Relativistic units mc^2 and mc for energy and momentum are used. The metric is such that the product of two four-vectors $\mathbf{a} = (a_0, \boldsymbol{a})$ and $\mathbf{b} = (b_0, \boldsymbol{b})$ is defined by $(ab) = a_0 b_0 - (\boldsymbol{a} \cdot \boldsymbol{b})$.

0340-4811 / 85 / 1200-1182 $ 01.30/0. – Please order a reprint rather than making your own copy.

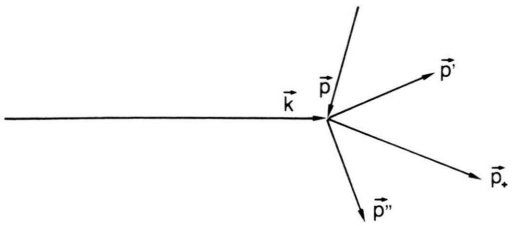

Fig. 1. Elementary process of pair production in the field of an electron.

collides with an electron with four-momentum $\mathbf{p} = (\varepsilon, \boldsymbol{p})$ and creates an electron-positron pair with four-momenta $\mathbf{p}' = (\varepsilon', \boldsymbol{p}')$ and $\mathbf{p}_+ = (\varepsilon_+, \boldsymbol{p}_+)$. The recoiling electron (clearly, the recoiling electron and the pair electron are undistinguishable) has the four-momentum $\mathbf{p}'' = (\varepsilon'', \boldsymbol{p}'')$; its coordinates can be eliminated by means of the energy-momentum conservation

$$\mathbf{k} + \mathbf{p} = \mathbf{p}_+ + \mathbf{p}' + \mathbf{p}''. \tag{1}$$

According to the substitution law [1] the cross section for this process can be derived from the cross section of electron-positron bremsstrahlung where an electron and a positron with four-momenta $\mathbf{p}$ and $\mathbf{q}$, respectively, collide under the emission of a photon with four-momentum $\mathbf{k}$; the scattered particles have the four-momenta $\mathbf{p}'$ and $\mathbf{q}'$ [11]. It requires the following substitutions:

$$\begin{aligned} &(pk) \to -(pk) = -\varkappa, \quad (qk) \to (p'k) = \varkappa', \\ &(pq) \to -(pp') = -\tau. \end{aligned} \tag{2}$$

Defining

$$\begin{aligned} \varrho^2 &= (\mathbf{p}_+ + \mathbf{p}'')^2 = 2[(p_+ p'') + 1] \\ &= 2(\varkappa - \varkappa' - \tau + 1), \end{aligned} \tag{3}$$

the differential cross section has the form

$$\frac{\mathrm{d}^2\sigma}{\mathrm{d}\varepsilon'\,\mathrm{d}\Omega_{p'}} = \frac{\alpha r_0^2}{2\pi}\,\frac{p'}{\varkappa}\,\frac{\sqrt{\varrho^2 - 4}}{\varrho}\,\Sigma_t. \tag{4}$$

Here $\Omega_{p'}$ is the solid angle of the outgoing electron, $\alpha \approx 1/137$ is the fine-structure constant, $r_0 = e^2/mc^2$ is the classical electron radius, and the quantity

$$\Sigma_t = \frac{1}{\pi} \int A_t\,\mathrm{d}\Omega_{p_+} \tag{5}$$

is obtained from (A 1) and (A 2) of [11] taking into account the substitutions (2). Σ_t is a complicated function of the invariant products $\varkappa$, $\varkappa'$, and τ (see (2)). The cross section (4) gives the angular distributions of the outgoing electrons for a fixed electron energy ε'. It complements the cross section (6.9) of [10] representing the corresponding positron distributions. From the detailed structure of the functions Σ_t is can be seen that it is impossible to obtain $\mathrm{d}^2\sigma/(\mathrm{d}\varepsilon'\,\mathrm{d}\Omega_{p'})$ from $\mathrm{d}^2\sigma/(\mathrm{d}\varepsilon_+\,\mathrm{d}\Omega_{p_+})$ simply by substitutions, as pointed out by Haug [10]. This fact is demonstrated still more clearly by considering the analogous bremsstrahlung processes. In the electron-electron case the calculation of $\mathrm{d}^2\sigma/(\mathrm{d}\varepsilon_+\,\mathrm{d}\Omega_{p_+})$ corresponds to the integration of the fully differential cross section over the angles of the *outgoing* electron, whereas $\mathrm{d}^2\sigma/(\mathrm{d}\varepsilon'\,\mathrm{d}\Omega_{p'})$ corresponds to the integration over the angles of one of the *incoming* electrons.

3. Results

Motivated by experimental investigations of the triplet process [12, 13], Jarp and Mork [9] have computed various cross sections in the laboratory system by numerical integration using the Monte Carlo method. Their results for the positron distributions were reproduced with higher accuracy by Haug [10]. By means of the formulae of Section 2 this can now be performed for the electron distributions.

3.1 Doubly Differential Cross Section in the Laboratory System

In the laboratory system the target electron is at rest, i.e., $\boldsymbol{p} = 0$, $\varepsilon = 1$, and $\varkappa = (pk) = k$. Here the doubly differential cross section has the form

$$\sigma(\varepsilon', \theta') \equiv \frac{\mathrm{d}^2\sigma}{\mathrm{d}\varepsilon'\,\mathrm{d}(\cos\theta')} = \alpha r_0^2\,\frac{p'}{k}\,\frac{\sqrt{\varrho^2 - 4}}{\varrho}\,\Sigma_t, \tag{6}$$

where

$$\varrho^2 = 2[k + 1 - \varepsilon' - k(\varepsilon' - p'\cos\theta')] \tag{7}$$

and θ' is the angle between the momenta $\boldsymbol{k}$ and $\boldsymbol{p}'$ of the incident photon and the outcoming electron. The kinematics of the triplet production are determined by the condition $\varrho^2 \geqq 4$. Therefore, for a fixed value of θ' the boundaries of the energy ε' in the laboratory system are given by

$$\frac{k^2 - 1 - k\cos\theta'\,W}{(k+1)^2 - k^2\cos^2\theta'} \leqq \varepsilon' \leqq \frac{k^2 - 1 + k\cos\theta'\,W}{(k+1)^2 - k^2\cos^2\theta'}, \tag{8}$$

where the square root

$$W = (k^2 \cos^2 \theta' - 4k)^{1/2} \tag{9}$$

has to be real. This requirement yields the limits of $\cos \theta'$:

$$2/\sqrt{k} \leqq \cos \theta' \leqq 1. \tag{10}$$

Since the threshold of the triplet process in the laboratory system is $k = 4$, the quantity $2/\sqrt{k}$ is never greater than 1.

Figure 2 shows $\sigma(\varepsilon', \theta')$ for $k = 5.12$, i.e., the photon energy $h\nu = 2.616$ MeV, as a function of the electron energy ε' for various values of the angle θ'. The cross section is maximum for electrons emitted into forward direction $\theta' = 0$; at any angle θ' it decreases steeply near the boundaries (8) of the electron energy. A comparison with Figure 8 of Jarp and Mork [9], which is computed for the same parameters, demonstrates the higher accuracy of the present calculations. The bends in Jarp and Mork's curves near $\varepsilon' = 1.9$ are artifacts resulting from the integration procedure.

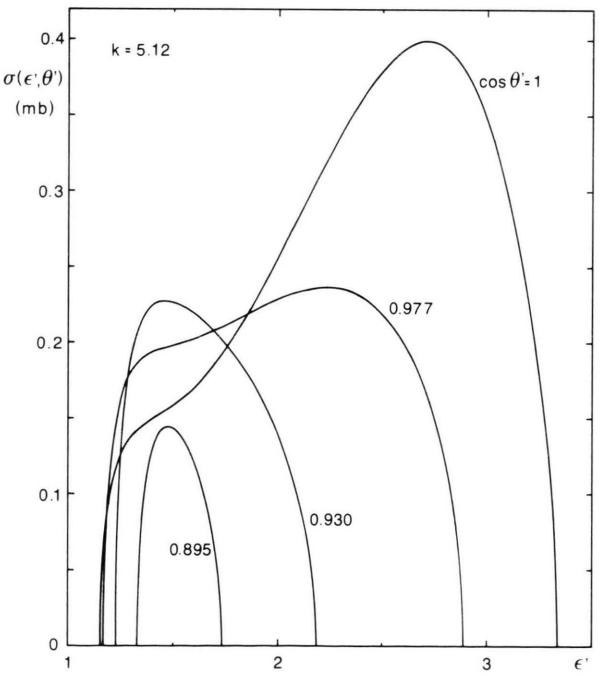

Fig. 2. Energy distributions of the outgoing electrons in the laboratory system for $k = 5.12$ and various angles θ'.

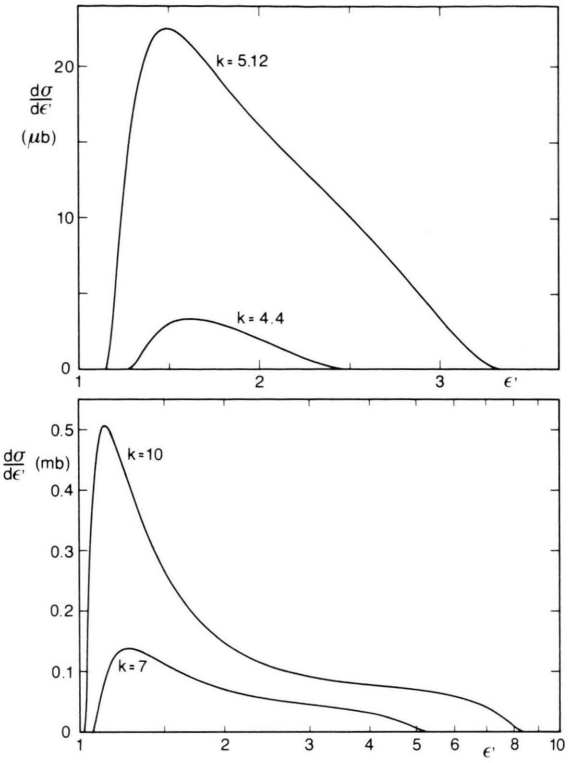

Fig. 3. Electron spectra in the laboratory system for the photon energies $k = 4.4$, 5.12, 7, and 10.

3.2. *Electron Energy and Angular Distributions in the Laboratory System*

The electron spectra $d\sigma/d\varepsilon'$ are obtained by a single numerical integration of the cross section $\sigma(\varepsilon', \theta')$ over $\cos \theta'$. For constant electron energy ε' the maximum angle θ'_M can be inferred from the condition $\varrho^2 \geqq 4$; from (7)

$$\cos \theta'_M = \frac{1}{p'} \left[\varepsilon' - 1 + \frac{\varepsilon' + 1}{k} \right] \leqq \cos \theta' \leqq 1. \tag{11}$$

For a given value of k the minimum and maximum energies, respectively, are obtained from (8) setting $\cos \theta' = 1$:

$$\varepsilon'_{m,M} = \frac{k^2 - 1 \mp k\,[k\,(k-4)]^{1/2}}{2k+1}. \tag{12}$$

The electron spectra for the photon energies $k = 4.4$, 5.12, 7.0, and 10 are plotted in Figure 3. Compared to the corresponding positron spectra which are

nearly symmetric about the average energy (see Fig. 12 of [10]), the maxima are shifted to lower energies ε'. This feature is most pronounced at the higher photon energies (note the logarithmic scale of the abscissa in the lower part of the figure). The larger values of the electron cross sections are due to the fact that the spectra refer to two (undistinguishable) electrons. Therefore the area under the electron spectra is twice the area under the positron spectra.

A comparison of Fig. 3 with the results of Jarp and Mork [9] shows again the increased accuracy reached by the present method with far less waste of computing time. Experimental cross sections are available only for $k = 5.12$ [13, 14]. At this energy the minimum momentum of the outgoing electrons (see (14) below) is of the order 1, i.e., the impact parameter is small so that the screening effects can be neglected in the triplet production on atomic electrons. In view of the low number of triplet events observed (50 and 314, respectively) the agreement between experimental and theoretical spectra is good.

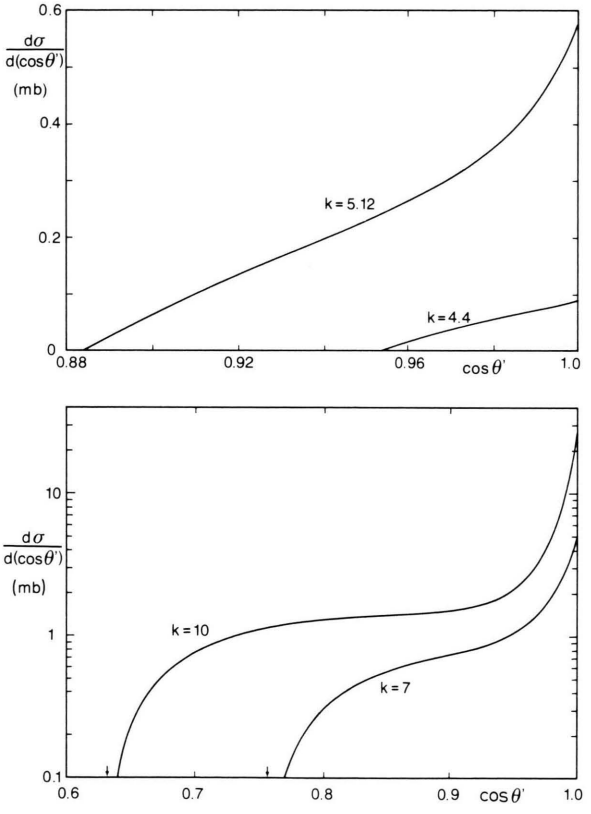

Fig. 4. Electron angular distributions in the laboratory system for the photon energies $k = 4.4$, 5.12, 7, and 10. The arrows at the lower abscissa give the boundaries of $\cos\theta'$.

With increasing photon energy the electron spectra become more and more asymmetric: nearly all the outcoming electrons have energies close to the lower boundary given by (12).

This behaviour originates from the fact that for large k the recoiling electron gets only a small energy. On the other hand the positron spectra for very high photon energies become nearly rectangular (see Fig. 13 of [10]).

The numerical integration of the cross section (6) over ε' yields the angular distribution $\mathrm{d}\sigma/\mathrm{d}(\cos\theta')$ of the electrons. The curves for photon energies $k = 4.4$, 5.12, 7, and 10 are shown in Fig. 4 as a function of $\cos\theta'$. As the photon energy increases the electrons are emitted predominantly into a more and more narrow cone in forward direction even though the kinematically allowed range of the angle θ' expands (see Eq. (10)). Figure 4 again verifies the distributions obtained by Jarp and Mork [9]. Comparing the angular distribution for $k = 5.12$ with the experimental results of Augerat et al. [13, 14] the same holds as above: there is good agreement within the uncertainties caused by the poor statistics of the measurements.

3.3 Electron Momentum Distribution in the Laboratory System

At high photon energies the most likely configuration in triplet production is that in which a pair with large momenta emerges in the near-forward direction and the second electron recoils at a relatively large angle with a small momentum [4]. In that case it is convenient to define this low-momentum electron as the "recoil electron". Since the two final electrons have very large separation in phase space, exchange can be neglected, i.e., the Borsellino approximation is expected to be good (the γ–e interaction gives also negligible contributions [4]). As soon as the two outgoing electrons have comparable momenta, the exchange effect will be important and differences between the present calculation and the Borsellino formula are expected. In particular this is true for low photon energies.

Choosing the particle with the primed coordinates $\varepsilon', \boldsymbol{p}'$ as the recoil electron, the recoil momentum distribution $\mathrm{d}\sigma/\mathrm{d}q$ can be easily obtained from

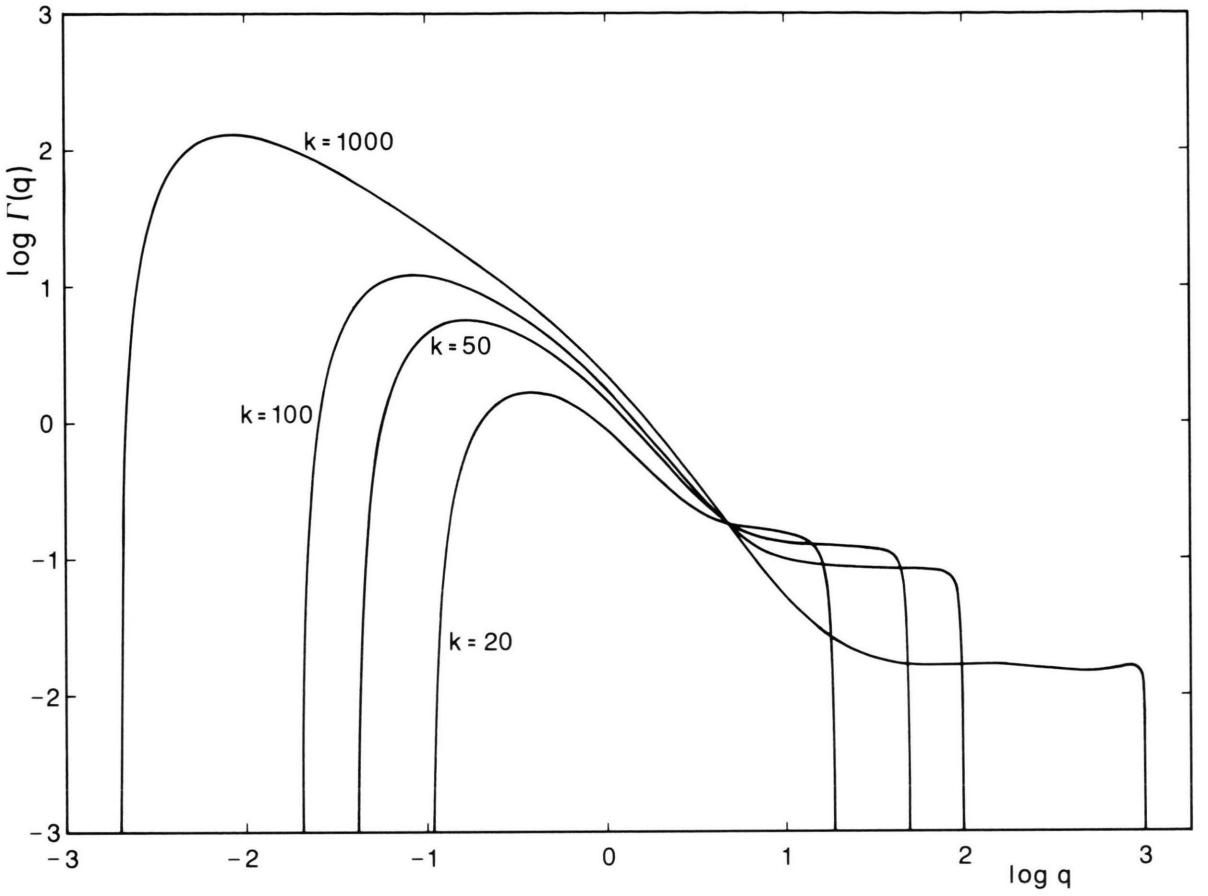

Fig. 5. Momentum distributions of the outgoing electrons in the laboratory system for $k = 20$, 50, 100, and 1000.

the energy distribution $\mathrm{d}\sigma/\mathrm{d}\varepsilon'$ by means of the relation $p'\,\mathrm{d}p' = \varepsilon'\,\mathrm{d}\varepsilon'$ (in the laboratory system $q = |\boldsymbol{p} - \boldsymbol{p}'| = p'$):

$$\frac{\mathrm{d}\sigma}{\mathrm{d}q} = \frac{p'}{\varepsilon'}\frac{\mathrm{d}\sigma}{\mathrm{d}\varepsilon'}. \tag{13}$$

The minimum and maximum recoil momenta, respectively, can be inferred from the corresponding energies (12) with the aid of the relation $q^2_{\mathrm{m,M}} = p'^2_{\mathrm{m,M}} = \varepsilon'^2_{\mathrm{m,M}} - 1$:

$$q_{\mathrm{m,M}} = \frac{k(k-1) \mp (k+1)\sqrt{k(k-4)}}{2k+1}. \tag{14}$$

Whereas near threshold ($k \approx 4$) $q_{\mathrm{m}} \approx q_{\mathrm{M}} \approx \frac{4}{3}$, the minimum recoil momentum tends to values $q_{\mathrm{m}} \ll 1$ for large photon energies:

$$q_{\mathrm{m}} \approx \frac{2}{k}\left(1 + \frac{1}{k}\right), \quad k \gg 1. \tag{15}$$

The computation of $\mathrm{d}\sigma/\mathrm{d}q$ from the differential cross section (6) requires one numerical integration over the angles θ'. The results are depicted in Fig. 5 which shows in a doubly logarithmic scale the normalized distributions

$$\Gamma(k, q) = \frac{1}{\alpha\, r_0^2}\frac{\mathrm{d}\sigma}{\mathrm{d}q} \tag{16}$$

for $k = 20$, 50, 100, and 1000. The cross sections are largest for small momenta $q < 1$. Nevertheless the contributions to the total cross section are approximately equal for $q_{\mathrm{m}} \leqq q \lesssim 1$ and for $1 \lesssim q \leqq q_{\mathrm{M}}$. This is in contrast to the behaviour of the recoil momentum distributions $\mathrm{d}\sigma_{\mathrm{Bors}}/\mathrm{d}q$ according to the Borsellino formula [5, 17] which are plotted in Mork's [8] Fig. 5 for the same values of k. A comparison shows that the two sets of curves agree for $q \lesssim 1$. At higher values of the recoil momentum,

however, the distribution of Borsellino decreases rapidly whereas the present curves flatten before they drop steeply close to q_M. This difference is due to the neglect of exchange in Borsellino's work.

Defining the momentum q_c by the condition

$$\int_{p_m}^{q_c} \frac{d\sigma}{dq} dq = \int_{q_c}^{q_M} \frac{d\sigma}{dq} dq, \tag{17}$$

the outgoing electrons with $q \leqq q_c$ can be designated as the recoil electrons and those with $q \geqq q_c$ as the pair electrons. For large photon energies q_c takes values of the order of one (e.g., $q_c = 0.92$ for $k = 20$, $q_c = 0.52$ for $k = 100$).

The concept of the recoil electron and the momentum distribution $d\sigma/dq$ are of importance in the calculation of the incoherent cross section, i.e., the total cross section for pair production in the field of Z *atomic* electrons, by means of the incoherent scattering function $S(q)$ [15–18]

$$\sigma_t(k, Z) = Z \int_{q_m}^{q_c} \frac{d\sigma}{dq} S(q)\, dq. \tag{18}$$

This expression can be split into two terms [18]:

$$\sigma_t(k, Z) = Z \left\{ \int_{q_m}^{q_c} \frac{d\sigma}{dq} dq - \int_{q_m}^{q_c} \frac{d\sigma}{dq} [1 - S(q)]\, dq \right\}. \tag{19}$$

According to (17), the first term represents the total cross section for triplet production in the field of *free* electrons,

$$\sigma_t(k) = \frac{1}{2} \int_{q_m}^{q_M} \frac{d\sigma}{dq} dq, \tag{20}$$

where the factor $\frac{1}{2}$ corrects for the double counting of the outgoing electrons. The second term in (19) is called the "screening correction" $\Delta S(k, Z)$ [18]. Atomic binding affects only the electrons with small values of q whereas for large q the recoil electrons receive sufficient energy to be considered free. As a result the incoherent scattering function $S(q)$ is very close to its asymptotic value $S(\infty) = 1$ for $q > q_0$, where $q_0 \ll 1$ (for hydrogen atoms, e.g., $S(q) > 0.999$ for $q > 0.031$). Therefore the upper limit q_c in the second integral of (19) can be replaced with q_0. Besides, the cross section $d\sigma/dq$ is equal to $d\sigma_{Bors}/dq$ in the small-q region; hence the total cross section (19) can be written as

$$\sigma_t(k, Z) = Z\{\sigma_t(k) - \Delta S(k, Z)\} \tag{21}$$

with

$$\Delta S(k, Z) = \int_{q_m}^{q_0} \frac{d\sigma_{Bors}}{dq} [1 - S(q)]\, dq. \tag{22}$$

The present derivation of (21), previously obtained by Maximon and Gimm [17, 18], shows that the failure of the Borsellino formula for $q \gtrsim 1$ does not affect the accuracy of the computation of $\sigma_t(k, Z)$. As can be seen from Fig. 9 of [17] (to which the reader is referred for a more detailed comparison with experiments) the agreement of the total cross section for pairs, computed with the aid of (21) for hydrogen, with experimental data is good.

4. Total Cross Section for Triplet Production

The total cross section for triplet production in the field of free electrons (20) can easily be computed from $\sigma(\varepsilon', \theta')$ by two numerical integrations:

$$\sigma_t = \frac{1}{2} \int_{\varepsilon_m'}^{\varepsilon_M'} \int_{\cos\theta_M'}^{1} \frac{d^2\sigma}{d\varepsilon'\, d(\cos\theta')} d\varepsilon'\, d(\cos\theta'), \tag{23}$$

where the integration limits are given by (11) and (12). If $\sigma(\varepsilon', \theta')$ is first integrated over the angle θ', the strong beaming of the electrons near forward direction is insignificant because, according to (11), the range of kinematically allowed angles θ' becomes very small at high energies k and ε'.

Since σ_t is a relativistic invariant, it is a function of the scalar product $\varkappa = (pk)$ which in the laboratory system reduces to the photon energy k. The threshold for the triplet process is at $(pk) = 4$. The cross sections obtained from (23) are identical to those obtained by numerical integration of the positron distributions [10], verifying the correctness of the expression Σ given in [11]. At high photon energies it is, however, preferable to compute σ_t by means of the positron distributions since the positron spectra are smoother functions of the energy than the electron spectra.

A table with values of σ_t for $4.001 \leqq k \leqq 5000$ are given in [10], where also comparisons with previous calculations can be found. Besides, the total cross section for triplet production has been fitted to simple analytic expressions by Haug [19].

[1] J. M. Jauch and F. Rohrlich, The Theory of Photons and Electrons, 2nd ed., Springer-Verlag, Berlin 1976.
[2] H. A. Bethe and W. Heitler, Proc. Roy. Soc. London A **146,** 83 (1934).
[3] V. Votruba, Phys. Rev. **73,** 1468 (1948); Bull. Intern. Acad. Tcheque Sci. **49,** 19 (1948).
[4] J. Joseph and F. Rohrlich, Rev. Mod. Phys. **30,** 354 (1958).
[5] A. Borsellino, Nuovo Cim. **4,** 112 (1947); Rev. Univ. Nac. Tucumán A **6,** 7 (1947).
[6] A. G. Ghizzetti, Rev. Univ. Nac. Tucumán A **6,** 37 (1947).
[7] G. I. Kopylov, L. A. Kulyukina, and I. V. Polubarinov, Sov. Phys. JETP **19,** 1158 (1964).
[8] K. J. Mork, Phys. Rev. **160,** 1065 (1967).
[9] S. Jarp and K. J. Mork, Phys. Rev. D **8,** 159 (1973).
[10] E. Haug, Z. Naturforsch. **30a,** 1099 (1975).
[11] E. Haug, Phys. Rev. D **31,** 2120 (1985).
[12] G. Roche, J. Arnold, J. Augerat, L. Avan, M. Avan, J. Bonnet, J. Fargeix, A. Fleury, J. Jousset, M. J. Parizet, and M. Vialle, Nucl. Instrum. Methods **103,** 533 (1972).
[13] J. Augerat, M. Avan, M. Ballet, J. Jousset, M. J. Parizet, and G. Roche, Lett. Nuovo Cim. **11,** 685 (1974).
[14] J. Augerat, M. Avan, M. J. Parizet, G. Roche, J. Arnold, J. Fargeix, and A. Fleury, Phys. Rev. A **15,** 1068 (1977).
[15] J. A. Wheeler and W. E. Lamb, Phys. Rev. **55,** 858 (1939); Erratum: Phys. Rev. **101,** 1836 (1956).
[16] K. S. Suh and H. A. Bethe, Phys. Rev. **115,** 672 (1959).
[17] L. C. Maximon and H. A. Gimm, Phys. Rev. A **23,** 172 (1981).
[18] H. A. Gimm, Phys. Rev. A **25,** 823 (1983).
[19] E. Haug, Z. Naturforsch. **36a,** 413 (1981).